



HAL
open science

Kinetic modeling of polyurethane pyrolysis using non-isothermal thermogravimetric analysis

Ghassan Jomaa, Patrick Goblet, Christophe Coquelet, Morlot Vincent

► To cite this version:

Ghassan Jomaa, Patrick Goblet, Christophe Coquelet, Morlot Vincent. Kinetic modeling of polyurethane pyrolysis using non-isothermal thermogravimetric analysis. *Thermochimica Acta*, 2015, 612, pp.10-18. 10.1016/j.tca.2015.05.009 . hal-01158620

HAL Id: hal-01158620

<https://minesparis-psl.hal.science/hal-01158620>

Submitted on 12 Jan 2016

HAL is a multi-disciplinary open access archive for the deposit and dissemination of scientific research documents, whether they are published or not. The documents may come from teaching and research institutions in France or abroad, or from public or private research centers.

L'archive ouverte pluridisciplinaire **HAL**, est destinée au dépôt et à la diffusion de documents scientifiques de niveau recherche, publiés ou non, émanant des établissements d'enseignement et de recherche français ou étrangers, des laboratoires publics ou privés.

Accepted Manuscript

Title: Kinetic modeling of polyurethane pyrolysis using non-isothermal thermogravimetric analysis

Author: Ghassan JOMAA Patrick GOBLET Christophe COQUELET Vincent MORLOT



PII: S0040-6031(15)00205-1
DOI: <http://dx.doi.org/doi:10.1016/j.tca.2015.05.009>
Reference: TCA 77228

To appear in: *Thermochemica Acta*

Received date: 29-11-2014
Revised date: 11-5-2015
Accepted date: 12-5-2015

Please cite this article as: Ghassan JOMAA, Patrick GOBLET, Christophe COQUELET, Vincent MORLOT, Kinetic modeling of polyurethane pyrolysis using non-isothermal thermogravimetric analysis, *Thermochemica Acta* (2015), <http://dx.doi.org/10.1016/j.tca.2015.05.009>

This is a PDF file of an unedited manuscript that has been accepted for publication. As a service to our customers we are providing this early version of the manuscript. The manuscript will undergo copyediting, typesetting, and review of the resulting proof before it is published in its final form. Please note that during the production process errors may be discovered which could affect the content, and all legal disclaimers that apply to the journal pertain.

Kinetic modeling of polyurethane pyrolysis using non-isothermal thermogravimetric analysis

Ghassan JOMAA^{a,c}, Patrick GOBLET^{a,*}, Christophe COQUELET^b, Vincent MORLOT^c

^a*MINES ParisTech, PSL Research University, Centre de Géosciences, 35 rue Saint Honoré 77305 Fontainebleau, France*

^b*Mines ParisTech, PSL Research University, CTP-Centre of Thermodynamic of Processes, 35 rue Saint Honoré 77305 Fontainebleau, France*

^c*Équipe Recherche et Développement, MONTUPET S.A., 3 rue de Nogent, 60290 Laigneville, France*

Abstract

The pyrolysis of polyurethane was studied by dynamic thermogravimetry analysis (TGA). The studied polyurethane is used as organic binder in casting process to make sand cores and molds. A semi-empirical model is presented that can be used to describe polyurethane pyrolysis occurring during TGA experiments. This model assumes that the polyurethane is pyrolysed by several parallel independent reactions. The kinetic parameters of polyurethane pyrolysis were evaluated by fitting the model to the experimental data obtained by TGA over a wide variety of heating rates. A nonlinear least-squares optimization method is employed in the fitting procedure. A hybrid objectives based simultaneously on the mass (TG) and mass loss rate (DTG) curves has been used in the least-squares method. The values of the activation energy obtained by the nonlinear fitting were then recalculated by the methods of Kissinger and Friedmand. Furthermore, the parameters obtained in the present paper were then compared with those reported in the literature.

Keywords:

kinetic parameters, polyurethane, pyrolysis, thermogravimetry, kinetic modeling

1. Introduction

1 Polyurethane is widely used in foundry industry as an organic binder to harden sand cores.
2 The latter are inserted into a metallic mold to obtain internal shapes of casting parts. Pouring of
3 a molten metal into the mold causes the thermal decomposition of polyurethane and gas emis-
4 sions which can represent a severe problem for the quality of the casting parts. Indeed, under the
5 effect of the thermal decomposition of the polyurethane, the pressure of the cores increases (due
6 to the produced gas). If the local gas pressure in the sand cores exceeds the local metallostatic
7 pressure of the solidifying liquid metal at core-casting part interface, gas bubbles can grow into
8 the metal. Depending on whether the gas bubbles escapes through the metal or not, two possible
9 scenarios can occur. In the first one the gas can escape through the casting part, so its effect might

*. Corresponding author

Email address: patrick.goblet@mines-paristech.fr (Patrick GOBLET)

10 be limited to the formation of bubble trails defect [1, 2]. In the second one, the gas bubbles stay
11 entrapped within the solidified metal. The entrapped gas bubbles contribute thus to the formation
12 of blowholes defects in the casting. Both bubble trails and blowholes defects affect the quality of
13 the casting parts by deteriorating their mechanical properties and thus these parts are generally
14 rejected. Nowadays, in order to prevent casting defects caused by the gas emissions and to assure
15 the soundness of castings, one can use numerical simulation which allows the determination of
16 the velocity and the pressure of the gas in the sand cores. The models used in the numerical simu-
17 lation of gas emissions are based on differential equations which describe the transport of mass,
18 momentum and energy within the sand cores. These equations contain source terms including
19 the thermal decomposition rate of the organic binder which are calculated using an appropriate
20 kinetic model. The reaction scheme and the parameters of the kinetic model have to be deter-
21 mined experimentally. Therefore, the study of the thermal decomposition of the polyurethane
22 represents a necessary step for the numerical simulation of the gas emissions occurring during
23 the pouring and the solidification of the casting parts.

24 Generally after pouring the molten metal into the mold, the sand cores are totally covered by
25 the metal. As there is no oxygen within the sand cores, the thermal decomposition of the poly-
26 urethane binder can be assumed to be done only by pyrolysis [2]. One of the most common used
27 thermal analysis techniques to study pyrolysis kinetics of organic solids is the thermogravimetry
28 analysis (TGA) [3]. TGA technique consists in measuring the mass of a substance as a function
29 of temperature (or time) while the substance is subjected to a controlled temperature programme.
30 The thermogravimetry analysis of a solid matter can be conducted either at isothermal conditions
31 (constant temperature) or non-isothermal/dynamics conditions (generally the temperature varies
32 linearly with time). The investigation of the pyrolysis by TGA is carried out in inert atmosphere
33 such as nitrogen, argon or Helium. However, one can study combustion by using a reactive at-
34 mosphere such as oxygen or hydrogen. The results obtained by TGA are principally the curves of
35 mass loss (noted TG) and of rate of mass loss (note DTG) as functions of temperature (or time).

36 Even though several works have been carried out to determine the kinetic parameters of the
37 pyrolysis of polyurethanes used in applications other than the foundry [4], only experimental
38 results have been reported about the pyrolysis of polyurethanes used in foundry [5-7]. The ob-
39 jective of this work is to propose a kinetic model of the polyurethane pyrolysis and to calculate
40 the kinetic parameters using TG and DTG curves obtained by thermogravimetry analysis of po-
41 lyurethane. The determined kinetic parameters could be used later within a computational fluid
42 dynamics model for gaseous emissions occurring in sand core during casting process [8].

2. Experimental results

43 The polyurethane binder studied in this work was prepared by the reaction of phenolic resin
44 and polyisocyanate resin. Both resins are in a liquid form and in combination with organic sol-
45 vents. A blend of an equal weight of phenolic and polyisocyanate resins were mixed to form a
46 reaction mixture. The formation of polyurethane occurred in the presence of a gaseous amine cat-
47 alyst (dimethylethanolamine). The obtained solid polyurethane was ground using a mortar and
48 pestle. Three samples were prepared with initial masses of 16.7, 16.0 and 16.4 mg. The analyses
49 of the samples were conducted by a Perkin-Elmer TGA 7 thermobalance. The samples were hea-
50 ted in nitrogen flow at different heating rates : 20, 60 and 80 °C min⁻¹. The mass loss and the
51 mass loss rate curves of the polyurethane are given in figure 1. The results shows that the average
52 value of the residual mass of polyurethane equals around 26.75 % of initial mass of the various
53 samples.

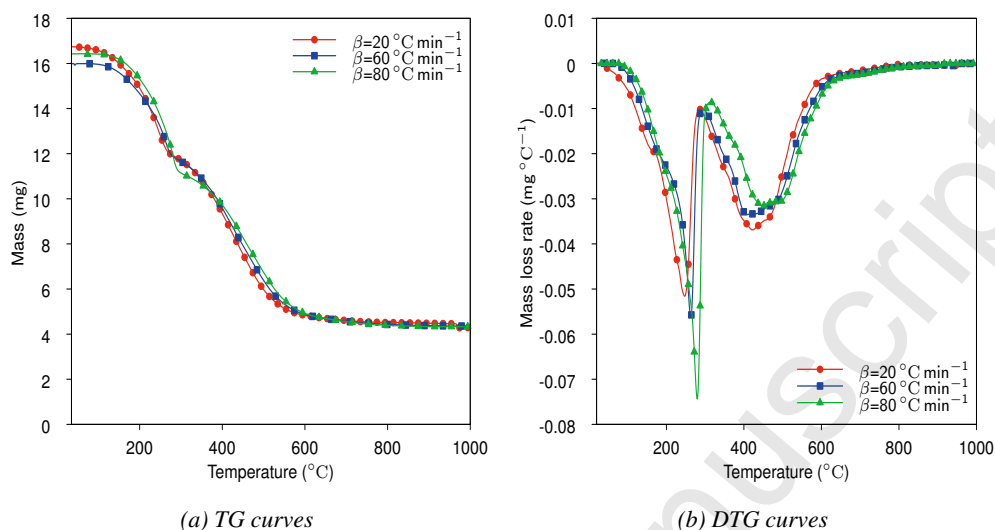


FIGURE 1: Experimental data of polyurethane pyrolysis obtained by TGA analysis conducted in nitrogen atmosphere and at various heating rates : 20, 60 and 80 °C min⁻¹

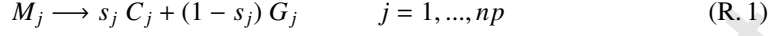
3. Kinetic Models of organic solid pyrolysis

There are abundance of published research works dealing with the modeling of the pyrolysis of solid matter using TGA. In these works, several kinetic models were employed to describe the pyrolysis of organic solids. We can mention among the used kinetic models : the single global reaction model [9–12], the parallel independent reactions model [13–17], and the distributed activation energy model [18–22]. In the single global reaction model, the pyrolysis of organic solid is described by only one reaction. This model is the simplest kinetic model that one can use. It is generally employed to describe thermal decomposition of a pure homogeneous solid. The parallel reaction model assumes that the organic solid is constituted of many solid fractions (pseudo-components) each of which is decomposed independently by one reaction. Therefore, the interaction of pyrolysis reactions of different pseudo-components is neglected. This model is essentially used to describe the pyrolysis of organic solid blends and mixtures. In the distributed activation energy model, the organic matter is assumed to be decomposed by an infinite number of parallel independent reactions. Each reaction has its own activation energy and the sum of all reactions is given by a distributed activation energy. This model is used generally to take into account the heterogeneity of the studied solid matter.

4. Kinetic Model of polyurethane pyrolysis

In this section, the kinetic model used in our study to describe polyurethane pyrolysis will be presented. This model is based on a parallel independent reactions model. In this model, the organic solid, noted M , will be considered as a mixture of np pseudo-components, noted M_j . The pseudo-components are supposed to decompose independently from one another, and not to

73 influence each other. The pyrolysis of each pseudo-component produces a gas noted G_j and a
74 solid noted C_j . Therefore the pyrolysis of M could be described by the reaction scheme R. 1.



75 Where s_j is the mass-based stoichiometric coefficient of pyrolysis reaction of solid pseudo-
76 component M_j . np is the number of parallel reactions. The conversion rate of each reaction j is
77 given by the following equation :

$$\frac{d\alpha_{M_j}}{dt} = k_j (1 - \alpha_{M_j})^{n_j} \quad j = 1, np \quad (1)$$

78 Where n_j is the order of the reaction. α_{M_j} is the conversion ratio of pyrolysable part of
79 pseudocomponent M_j . It is defined as :

$$\alpha_{M_j} = \frac{m_{M_j}^0 - m_{M_j}}{m_{M_j}^0 - m_{M_j}^\infty} \quad j = 1, \dots, np \quad (2)$$

80 Where $m_{M_j}^0$ is the initial mass of M_j . m_{M_j} the mass of M_j during the pyrolysis reaction. $m_{M_j}^\infty$
81 is the final mass of M_j when the reaction is complete.

82 The kinetic coefficients k_j are function only of temperature. k_j are given in an Arrhenius
83 form :

$$k_j = Z_j \exp\left(\frac{-Ea_j}{RT}\right) \quad j = 1, np \quad (3)$$

84 Where Z_j , Ea_j and R are the pre-exponential factors, activation energies, and the universal
85 gas constant, respectively. The overall conversion rate of the solid matter M is given by a linear
86 combination of conversion rates of M_j and, is expressed by the equation (4).

$$\frac{d\alpha_M}{dt} = \sum_{j=1}^{np} c_j Z_j \exp\left(\frac{-Ea_j}{RT}\right) (1 - \alpha_{M_j})^{n_j} \quad (4)$$

87 Where the coefficient c_j represents the fraction of the overall mass loss due to the pseudo-
88 component M_j . The sum of these coefficients has to be equal to unity :

$$\sum_{j=1}^{np} c_j = 1 \quad (5)$$

89 In the same way, the conversion ratio of the solid matter M is given by a linear combination
90 of conversion ratio of different pseudo-components M_j :

$$\alpha_M = \sum_{j=1}^{np} c_j \alpha_{M_j} \quad (6)$$

91 α_M can be calculated using TGA results by the following equation :

$$\alpha_M = \frac{m_M^0 - m_M}{m_M^0 - m_M^\infty} \quad (7)$$

92 m_M^0 , $m_{M_j}^\infty$ and m_{M_j} are the initial, final and current weights of M . If we consider that the
 93 TGA experiments have been carried out in non-isothermal conditions, the conversion rate of the
 94 organic matter M might be written as :

$$\frac{d\alpha_M}{dt} = \frac{dT}{dt} \frac{d\alpha_M}{dT} = \beta \frac{d\alpha_M}{dT} \quad (8)$$

95 Therefore, we have :

$$\frac{d\alpha_M}{dT} = \frac{1}{\beta} \sum_{j=1}^{np} c_j Z_j \exp\left(\frac{-Ea_j}{RT}\right) (1 - \alpha_{M_j})^{n_j} \quad (9)$$

96 where $\beta = dT/dt$ is the heating rate of sample during the TGA experiments. If the sample
 97 is subjected to a linear temperature ramp, the temperature can be expressed by the following
 98 equation :

$$T = \beta t + T^0 \quad (10)$$

99 Where t is time and T^0 is the initial temperature of the sample. For each reaction, there are
 100 four kinetic parameters (c_j , Z_j , Ea_j and n_j).

101 Using the definition of ratio conversion α_M given by the equation (7), the rate conversion of
 102 M can be evaluated by equation (11).

$$\frac{d\alpha_M}{dT} = \frac{-1}{m_M^0 - m_M^\infty} \frac{dm_M}{dT} \quad (11)$$

103 If we consider also np as an unknown, the model would have $4 \times np + 1$ kinetic parameters
 104 which have to be determined by fitting kinetic model equations to experimental data obtained by
 105 TGA.

5. Determination of kinetic parameters

106 There are several methods for determining the kinetic parameters of the pyrolysis of solid
 107 materials. We may classify them as linear and nonlinear methods. It is worthy to note that this
 108 classification is based upon the mathematical analysis of the experimental results. An classifica-
 109 tion according to experimental conditions of pyrolysis analysis such as isothermal and non-
 110 isothermal may be also used [23].

5.1. Linear Methods

111 These methods consist of finding a linear relationship between the kinetic parameters using
 112 the reaction rate given by the considered kinetic model. Then using the experimental results the
 113 coefficients of the linear relation are determined by a linear regression. Those method are gene-
 114 rally applied for a simple kinetic model in which the solid material is supposed to be decomposed
 115 in a single step. It is so described by one elementary reaction. This is the case where we have
 116 one reaction in the pyrolysis model presented above. In this case the reaction rate is given by the
 117 following equation :

$$\frac{d\alpha_M}{dT} = \frac{Z}{\beta} \exp\left(\frac{-Ea}{RT}\right) (1 - \alpha_M)^n \quad (12)$$

118 This expression of reaction rate is used when the reaction mechanism is characterized by a
 119 homogeneous chemical kinetic [24]. For more general case of other reaction mechanisms, the
 120 reaction rate can be expressed as shown below :

$$\frac{d\alpha_M}{dT} = \frac{Z}{\beta} \exp\left(\frac{-Ea}{RT}\right) f(\alpha_M) \quad (13)$$

121 Where $f(\alpha_M)$ is the reaction function which can take many mathematical forms depending
 122 on the controlling reaction mechanism. For example, some forms of this function can be found
 123 in [23, 25–30].

124 Many linear methods have been reported in the literature [23, 30–34]. The Friedman and
 125 Kissinger Methods are presented above.

5.1.1. Friedman Method

126 This method was introduced by Friedman [35]. The linear relationship employed by this
 127 method is obtained by taking the logarithm of the equation (13) which leads to the expression
 128 (14).

$$\ln\left(\beta \frac{d\alpha_M}{dT}\right) = \ln Z + \ln f(\alpha_M) - \frac{Ea}{RT} \quad (14)$$

129 For a given conversion degree α_M , plotting $\ln\left(\beta \frac{d\alpha_M}{dT}\right)$ as a function of $\frac{1}{T}$ for several heating
 130 rates yields a straight line whose slope is equal to $-\frac{Ea}{R}$. Therefore the activation energy of the
 131 reaction Ea is obtained from the slope. We note that the estimation of the activation energy by
 132 Friedman method does not require to know the reaction function $f(\alpha_M)$. This is why this method
 133 is considered as a free-model method. In order to estimate the pre-exponential factor Z from the
 134 y-intercept of the straight line, the function $f(\alpha_M)$ must be known.

5.1.2. Kissinger Method

135 This method was firstly introduced by Kissinger [36]. It is based on the temperature of the
 136 maximum rate of conversion (temperature of peaks in DTG). Indeed, the derivative of the conver-
 137 sion rate is equal to zero at the peak temperature of the DTG curve. The derivative of the conver-
 138 sion rate is given by the equation (15).

$$\frac{d^2\alpha_M}{dT^2} = \left[\frac{Ea}{RT^2} + \frac{Z}{\beta} \exp\left(\frac{-Ea}{RT}\right) \frac{df(\alpha_M)}{d\alpha_M} \right] \frac{d\alpha_M}{dT} \quad (15)$$

139 If we assume that the maximum reaction rate occurs at the peak temperature T_{max} , as the
 140 derivative of the conversion rate at T_{max} is equal to zero, we obtain the following equation :

$$\frac{Ea}{RT_{max}^2} - \frac{mZ}{\beta} \exp\left(\frac{-Ea}{RT_{max}}\right) = 0 \quad (16)$$

141 Which may also be rearranged in the following form

$$\frac{\beta}{T_{max}^2} = \frac{mZ}{Ea} \exp\left(\frac{-Ea}{RT_{max}}\right) \quad (17)$$

142 Where $m = -\frac{df(\alpha_M)}{d\alpha_M}|_{T=T_{max}}$. Taking the logarithm of this equation leads to the linear relation-
143 ship of Kissinger :

$$\ln\left(\frac{\beta}{T_{max}^2}\right) = \ln\left(\frac{m Z R}{Ea}\right) - \frac{Ea}{RT_{max}} \quad (18)$$

144 For a set of DTG curves with different heating rates β , the plot of $\ln\left(\frac{\beta}{T_{max}^2}\right)$ as a function of
145 $\frac{1}{T_{max}}$ would lead to a straight line whose slope $\frac{-Ea}{R}$ gives the activation energy. Kissinger method
146 is also considered as model-free method. If the form of the function $f(\alpha_M)$ is known, the pre-
147 exponential factor Z constant can be further determined from the y-intercept of the obtained
148 straight line.

5.2. Non-linear Methods

149 This type of methods is based on nonlinear least-square regression [37–42]. The kinetic pa-
150 rameters are calculated in this method by minimizing an objective function based on the sum of
151 weighted square of the error between the experimental data of thermogravimetry analysis and
152 model equations. These methods allow a direct fitting of the model equations to the experimental
153 data without any rearrangement or approximation. Moreover, they are robust methods to estimate
154 kinetic parameters of models with complex reaction schemes .

155 Depending on whether the conversion ratio or the conversion rate of the pseudo-compounds
156 is used, the objective function may be defined in two ways. In the first one, the objective function
157 is defined by the conversion ratio :

$$Of^I(\mathbf{a}) = 100 \times \sqrt{\sum_{l=1}^{N_{TGA}} \sum_{i=1}^{N_{exp}^l} \left[\frac{\alpha_M^{exp,l}(t_i) - \alpha_M^l(t_i, T_i, \mathbf{a})}{N_{exp}^l} \right]^2} \quad (19)$$

158 \mathbf{a} is the vector of the kinetic parameters to be estimated. It is defined as follows :

$$\mathbf{a} = \{Ea_1, \dots, Ea_{np}, Z_1, \dots, Z_{np}, c_1, \dots, c_{np}, n_1, \dots, n_{np}\}^T$$

159 N_{TGA} and N_{exp}^l are the numbers of TGA experiments and of points, respectively, in a given
160 experiment. Subscript l indicates the different experiments. $\alpha_M^{exp,l}(t_i)$ and $\alpha_M^l(t_i, T_i, \mathbf{a})$ denote the
161 experimental and estimated conversion ratios at instant t_i (temperature T_i). This form of the
162 objective function is called the integral form. The other form of the objective function is defined
163 based on the conversion rate equation :

$$Of^D(\mathbf{a}) = 100 \times \sqrt{\sum_{l=1}^{N_{TGA}} \sum_{i=1}^{N_{exp}^l} \left[\frac{\frac{d\alpha_M^{exp,l}(t_i)}{dt} - \frac{d\alpha_M^l(t_i, T_i, \mathbf{a})}{dt}}{N_{exp}^l \left. \frac{d\alpha_M^l(t_i)}{dt} \right|_{max}} \right]^2} \quad (20)$$

164 This form of the objective function is called the differential form. The division by $\left. \frac{d\alpha_M^{exp,l}(t_i)}{dt} \right|_{max}$
165 serves to normalize the conversion rate of different samples. In fact, since the TGA experiments
166 are carried out at different heating rates, the difference between the conversion rate of different
167 samples could be very important. Therefore, in order to consider the effect of all experiments
168 in the objective function, the conversion rate of each sample is divided by its maximum value
169 [43, 44].

170 It is important to note that both forms of the objective functions have been used in the li-
 171 terature to determine the kinetic parameters. Studies such as the ones of [15, 40, 45] and [46]
 172 have employed the integral form. As examples of studies that have used the differential form,
 173 we mention [16, 47, 48] and [49]. The difference between the estimation of kinetic parameters
 174 by the integral and differential forms of objective function have been rarely discussed in various
 175 publications. A discussion of the difference between these two forms was conducted by [22]. Ac-
 176 cording to Várhegyi et al. [22], it is somewhat difficult to determine the most appropriate form
 177 to determine the kinetic parameters. A good choice for the estimation of kinetic parameters of
 178 reactions with slow conversion rates would be the integral form. In other cases, the minimization
 179 of the differential form is the most sensible to estimate the kinetic parameters choice.

180 In this paper, we use a hybrid form of the objective function that simultaneously takes into
 181 account the minimization of both integral and differential forms (19) and (20). This hybrid form
 182 is given by the following function :

$$Of = \sqrt{(1 - \lambda)Of^I + \lambda Of^D} \quad (21)$$

183 where λ is a number varying between 0 and 1. When λ equals to 0, we get the integral form
 184 of objective function. When λ equals to 1, the form of the objective function is the differential
 185 one. In order to determine the kinetic parameters, the minimization of the objective function
 186 (21) has been achieved using the pattern search method of Hooke-Jeeves [50, 51] method. It is
 187 an iterative method of minimization which does not require the calculation of derivatives of the
 188 objective function. This method has been used by Várhegyi et al. [49] to determine the kinetic
 189 parameters. [49] has shown that even though this method converges slowly toward the optimal
 190 parameters, it is an efficient method.

191 The evaluation of the objective function requires the calculation of the conversion ratio and
 192 conversion rate of polyurethane pyrolysis. The calculation of these values was obtained by the
 193 numerical integration of the differential equations given by the equations of rate conversion of the
 194 different pseudo-components (Eq. 4). The integration is conducted by the fourth-order Runge-
 195 Kutta method.

6. Results and discussion

196 Figures 1 shows that the decomposition of the different samples starts at 100 °C. DTG curve
 197 illustrates clearly that the pyrolysis of polyurethane is occurring in at least two steps which
 198 correspond to the successive reactions of thermal decomposition of the polyol resins and the
 199 polyisocyanate resin. The first one takes place between 100 and 300 °C. About 50 % of the total
 200 decomposed mass of polyurethane is lost in the first step. The second one starts approximately
 201 at 300 and extends to 800 °C. Therefore, the polyurethane decomposes in a broader range in the
 202 second step. Otherwise, in this step about 50 % of total decomposed polyurethane is lost. It is
 203 important to note that the final char residue represents about 26.75 % of initial mass of samples.

6.1. Decomposition of polyurethane by two parallel independent reactions

204 In order to determine the kinetic parameters of polyurethane pyrolysis, we supposed firstly
 205 that the decomposition of the polyurethane is done by two parallel independent reactions. In
 206 other words, the decomposition of polyurethane in each step will be described by one reaction.
 207 As initial values for the kinetic parameters we have taken : 1×10^5 kJ mol⁻¹ for activation energy,
 208 1.0×10^{10} s⁻¹ for the pre-exponential factor, 0.5 for the coefficient c_j and 1 for the reaction order.

209 The parameter λ is set to 0.5. The optimized kinetic parameters for the polyurethane pyrolysis are
 210 shown in table 1. The final value of the objective function is 10.81 %. From the optimal coefficient
 211 c_j , we find that about 0.45 of the polyurethane is decomposed in the first stage while about 0.55 is
 212 decomposed during the second one. It is worth noting that as the sum of the c_j coefficient has to
 213 be equal to 1, the obtained values c_j have been normalized to satisfy this condition. These results
 214 may be explained by the fact that each stage represents the decomposition of one of the organic
 215 resins from which the polyurethane is synthesized. From the results, it can be seen also that the
 216 polyurethane pyrolysis has a reaction order close to two in the 2 step and to 3 in the second one.

TABLE 1: Kinetic parameters of polyurethane pyrolysis obtained using the Least-Squares Evaluation of three experiments

Reactions	c_j	c_j^{norm}	Z_j (s^{-1})	Ea_j ($kJ\ mol^{-1}$)	n_j	Of (%)
1	0.454	0.450	2.45×10^4	59.8	1.905	10.81
2	0.556	0.550	1.20×10^6	107.2	2.882	

217 Examples of comparison between the calculated and experimental results of polyurethane
 218 pyrolysis at the slowest and fastest heating rates, 20 and 80 $^{\circ}C\ min^{-1}$, are presented on the figure
 219 2. The figures show that the model can globally follow the shape of the peak temperatures in
 220 the different stages of polyurethane decomposition. However, the two reactions model could
 221 not determine accurately the position of the peaks along the temperature axis and their height.
 222 Moreover, the figures indicate that the model did not reproduce the shoulders appearing on the
 223 first and second stages of the DTG curves. We note that a shoulder represent generally a peak
 224 temperature which overlap another neighboring peak temperature [47].

6.2. Decomposition of polyurethane by four parallel reactions

225 It is somewhat difficult to describe each step by one reaction. That is why we have supposed
 226 that each step occurs by two parallel independent reactions highly overlapping each other. There-
 227 fore, the polyurethane pyrolysis is supposed to be done by four parallel independent reactions.
 228 In order to determine the kinetic parameters of these reactions by least square method, we chose
 229 equal initial values of the kinetics parameters : 0.25, $1.0 \times 10^{10}\ s^{-1}$, $1 \times 10^5\ kJ\ mol^{-1}$, 1 for c_j , Z_j ,
 230 Ea_j and n_j respectively. We take λ equal to 0.5. The initial value of the objective function equals
 231 103.47 %. The best value of the objective function obtained by the minimization process is about
 232 of 5.56 %. Table 2 shows the estimated kinetic parameters obtained from the pyrolysis of poly-
 233 urethane. Figure 3 shows the curves of the conversion ratio and conversion rate obtained by TGA
 234 analysis and the used kinetic model at the slowest and fastest heating rates : 20 and 80 $^{\circ}C\ min^{-1}$.
 235 We can observe a good agreement between experimental and calculated result. We note that the
 236 optimal objective function decreased from 10.81 % in the case of two reactions model to 5.56 %
 237 for the four reactions model. The decrease of the objective function proves that the latter one fits
 238 better the experimental data. The use of four reactions model allow to describe successfully the
 239 shoulders appearing in the DTG curves for both slowest and fastest heating rates. Furthermore,
 240 the four reactions model determined more precisely the position of the peaks along the tempera-
 241 ture axis. However, the fit still slightly inaccurate to describe the peak height especially for the
 242 fastest heating rate.

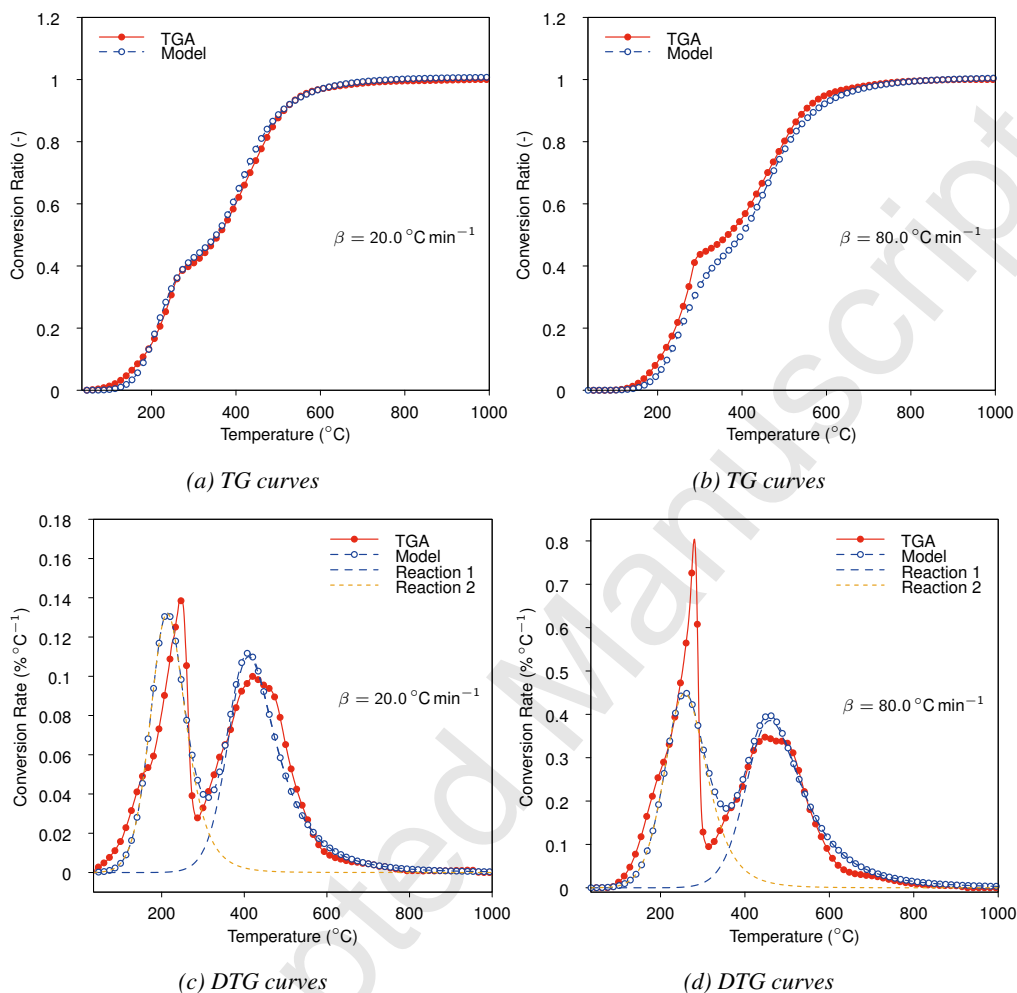


FIGURE 2: Experimental and calculated pyrolysis TG and DTG curves at the slowest and fastest heating rates, 20 and 80 °C min⁻¹, for 2-parallel independent reactions model

TABLE 2: Kinetic parameters of polyurethane pyrolysis obtained using the Least-Squares Evaluation of three experiments

Reactions	c_j	c_j^{norm}	Z_j (s ⁻¹)	Ea_j (kJ mol ⁻¹)	n_j	Of (%)
1	0.334	0.331	9.95×10^4	59.650	4.455	5.57
2	0.160	0.159	1.50×10^{10}	118.12	0.857	
3	0.235	0.233	3.187×10^7	117.09	2.336	
4	0.280	0.277	4.26×10^8	148.07	2.575	

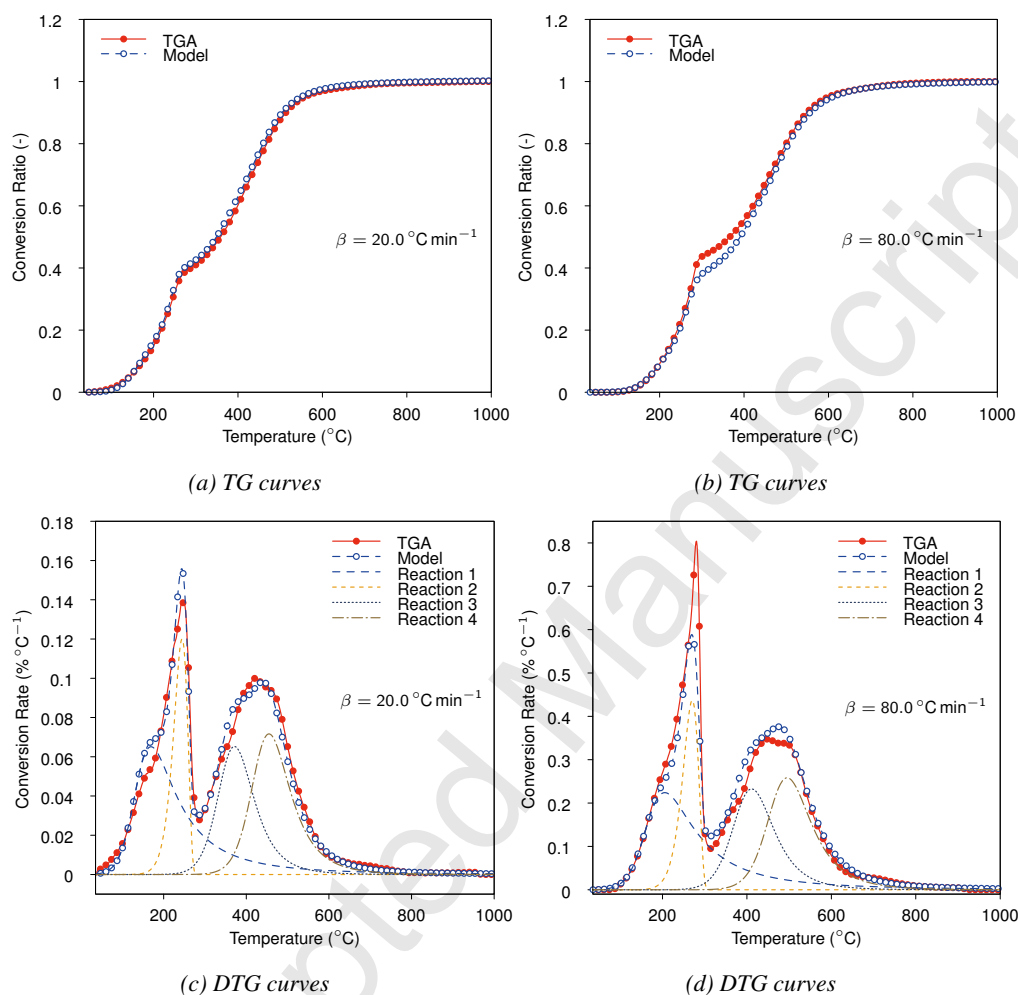


FIGURE 3: Comparison between experimental and calculated data at the slowest and fastest heating rates, 20 and 80 °C min⁻¹, for 4-parallel independent reactions model

6.3. Effect of thermal-lag on the kinetic analysis

243 In the above sections, we have taken the temperature of samples uniform and equal to the
 244 TGA furnace temperature. The latter one increases linearly as a function of time at the constant
 245 heating rate β (cf. eq.(10)). In reality, there is a thermal lag (deviation) between the true sample
 246 and furnace temperatures. Indeed, they could be equal only on the surface of the sample. Many
 247 papers have investigated thermal lag occurring during TGA analysis [52–56]. These papers
 248 reported that the thermal lag could be affected by many factors such as heating rate, initial
 249 size/mass of the sample, thermal effect of the reactions (heat generation/absorption by exothermic/endothermic reactions), the composition and the thermo-physical properties of the sample
 250 and the carrier gas of TGA, etc [52–55].

252 The temperature of the polyurethane samples was measured during the TGA measurements

253 conducted in the current study. Figure 4 shows that there is an important deviation between the
 254 measured and furnace temperatures (henceforth noted T_m and T_f respectively) for the three cho-
 255 sen heating rates 20, 60 and $80\text{ }^\circ\text{C min}^{-1}$. The maximum thermal lags ($T_m - T_f$) are equal to
 256 67.99, 86.81 and $87.70\text{ }^\circ\text{C}$ for these three heating rates respectively. The variation of the sample
 257 temperature as a function of time can be re-described by a linear relation with new heating rates
 258 which are 21.28, 65.46 and $88.15\text{ }^\circ\text{C min}^{-1}$. One can explain these higher thermal lags essentially
 259 by three factors which are the heating rates, initial mass of samples and the self-heating of the
 260 samples. Indeed as explained by many studies [52, 55], the thermal lag can dramatically increase
 261 with heating rate. Moreover, the use of an important initial sample mass can lead to the creation
 262 of temperature gradient and therefore to the increasing of thermal-lag (particularly at higher heating
 263 rates). It was recommended that the heating rate and the initial mass samples should be less
 264 than $10\text{ }^\circ\text{C min}^{-1}$ and 10 mg respectively in order to minimize the thermal-lag [54]. The violation
 265 of these recommendations in the measurements conducted in the current study (the initial mass
 266 of the samples are 16.7, 16.0 and 16.4 mg and the heating rates are 20, 60 and $80\text{ }^\circ\text{C min}^{-1}$ res-
 267 pectively) could explain the important thermal lag values occurring during TGA analyses. The
 268 third factor which can be noted from the positive deviation between the sample and the furnace
 269 temperatures is the self-heating. Indeed, as the temperature of the sample increases faster than
 270 that of the furnace, one can conclude that there is a heat generation occurring during polyurethane
 271 pyrolysis reaction (i.e. exothermic reaction). The self-heating of the sample can lead to a
 272 gradient temperature inside the sample (especially with higher initial mass) [54, 55]. To minimize
 273 the effect of the self-heating, one can use lower initial sample mass [55].

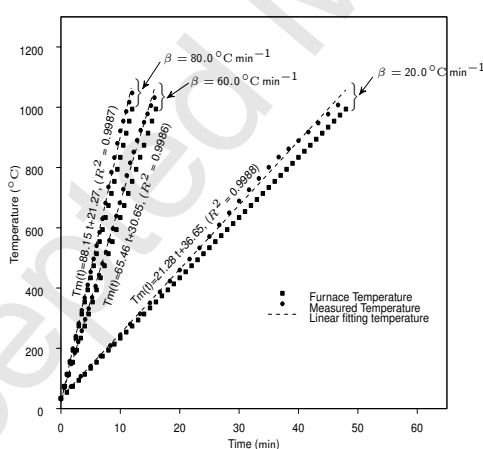


FIGURE 4: Variation of furnace and measured temperatures with respect to time at various heating rates :
 20, 60 and $80\text{ }^\circ\text{C min}^{-1}$

274 In order to illustrate the effect of the thermal lag on the kinetic analysis of polyurethane
 275 pyrolysis, we will recalculate the kinetic parameters of the two reactions model using the sample
 276 temperature obtained at the three heating rates 20, 60 and $80\text{ }^\circ\text{C min}^{-1}$. Even though we can use
 277 the new heating rates obtained by the linear regression of the sample temperature (67.99, 86.81
 278 and $87.70\text{ }^\circ\text{C}$) in the new kinetic analysis of polyurethane pyrolysis, we will use the raw values of
 279 the sample temperature measured by the thermocouple during the TGA experiments. The same
 280 initial values of the kinetic parameters used in the previous kinetic analysis with two reactions

281 model were used in the current one. The new optimized kinetic parameters were obtained for a
 282 objective function of 10.84 %. These parameters are shown in table 3. The new results of kinetic
 283 analysis of polyurethane pyrolysis illustrate that taking into account the thermal lag leads to
 284 different kinetic parameters. The new activation energies of the first and second reactions are
 285 greater than that obtained for the furnace temperature (60.5 and 110.6 kJ mol⁻¹ instead of 59.8
 286 and 107.2 kJ mol⁻¹ respectively). The exponential factor of the first reaction was decreased from
 287 2.24×10^4 to 2.45×10^4 s⁻¹, however that of second reaction was increased from 1.20×10^6 to
 288 1.22×10^6 s⁻¹. The orders of first and second reactions were increased to become 2.038 and
 289 3.022 instead of 1.905 and 2.882 respectively. One can also note that the objective function Of of
 290 the current kinetic analysis (has a value of 10.84 %) is just slightly higher than the one obtained
 291 in the case of use the furnace temperature (equals to 10.81 %).

292 The recalculation of the kinetic parameters using the sample temperature shows that the ac-
 293 curacy of the estimated parameters was severely affected by the thermal lag. In order to improve
 294 the accuracy of the kinetic analysis, new TGA experiments with lower heating rates and initial
 295 mass of samples should be done. Furthermore, the development of a more detailed heat transfer
 296 model within the sample will allow a more accurate kinetic analysis of polyurethane pyrolysis.

TABLE 3: Kinetic parameters of polyurethane pyrolysis calculated using the sample temperature

Reactions	c_j	c_j^{norm}	Z_j (s ⁻¹)	Ea_j (kJ mol ⁻¹)	n_j	Of (%)
1	0.463	0.458	2.24×10^4	60.5	2.038	10.84
2	0.547	0.542	1.22×10^6	110.6	3.022	

6.4. Estimation of activation energy by Kissinger's and Friedman's methods

297 A comparison was conducted between the kinetic parameters estimated by the non-linear and
 298 linear fitting methods. The values of activation energy of each step was determined by two linear
 299 methods, namely Kissinger and Friedman methods. Table 4 presents the energy of activation of
 300 polyurethane decomposition calculated by the different methods.

301 To determine the activation energy of each reaction by Kissinger method, T_{max}^2 is plotted as
 302 a function of $\frac{-1}{T_{max}}$ for the peak of each step at different heating rates. T_{max} is the temperature
 303 corresponding to the maximum rate of decomposition. As explained above, the resulting plot
 304 is a straight line whose slope is $\frac{Ea}{R}$. The estimated activation energy for the first and second
 305 steps are equal to 66.60 and 210.50 kJ mol⁻¹, respectively. The value of the square of correlation
 306 coefficient (r^2) is equal to 0.9667 for the first step and 0.8939 for the second one, which can
 307 indicate that the experimental data are well fitted by linear plot for the two steps.

308 The determination of activation energy by the Friedman method was carried out for two
 309 conversion degrees of 0.15 and 0.85 which are chosen to be in the first and second stage respec-
 310 tively. Plotting of $\ln\left(\beta\frac{d\alpha}{dT}\right)$ as a function of $\frac{1}{T}$ for each conversion degree leads to the estimated
 311 values of activation energy of 111.5 and 202.9 kJ mol⁻¹ for the first and second stage respec-
 312 tively. The square of the correlation coefficient of Friedman plot of the first and second stage are
 313 equals to 0.9999 and 0.9909 respectively.

314 The results show that the values of the activation energy obtained by the different methods are
 315 globally quite different. The values of the activation energies obtained by non-linear fitting are
 316 generally lower than those obtained by Kissinger and Friedman methods. However, the value of
 317 activation energy obtained for the first stage using the non-linear fitting method (59.80 kJ mol⁻¹)

TABLE 4: Activation energies of polyurethane decomposition estimated by the different methods

Methods	Ea_1 (kJ mol ⁻¹)	Ea_2 (kJ mol ⁻¹)
Non-linear	59.80	107.2
Kissinger	66.60	210.5
Friedman	115.5	202.9

is close to that obtained by Kissinger method (66.60 kJ mol⁻¹). For the second stage, the values obtained by the Kissinger and Friedman methods are quite similar, 210.5 and 202.9 kJ mol⁻¹ respectively. The difference between the results obtained by the different methods may be attributed to the dissimilar mathematical treatment in each method.

6.5. Comparison of current results with published ones

Many studies have investigated the pyrolysis of polyurethane. A comparison between of the estimated kinetic parameters published in the literature and those obtained by the current study is given in table 5. Different types of polyurethane have been analyzed in this studies. Font et al [12] studied the pyrolysis of commercial polyurethane obtained by the reaction between the polyadipate of 1,4-butanediol or 1,6-hexanediol with diphenylmethane p,p'-diisocyanate. Rein et al [57] studied the flexible polyurethane foam. Prasad et al [58] studied polyurethane foam formed out of a reaction between toluene diisocyanate (TDI) and a polyol. Pau et al [59] studied polyurethane foams made from the reaction of mainly toluene diisocyanate and polyalkoxy polyether polyol.

TABLE 5: Comparison between the kinetic parameters of polyurethane pyrolysis obtained in this work with other published results

	Ea_j (kJ mol ⁻¹)	Z_j (s ⁻¹)	n_j
Font et al [12]	133.6	2.55×10^{12}	0.951
	190.4	9.76×10^{15}	0.668
Rein et al [57]	124.0	1.58×10^8	1.140
	148.0	2.00×10^{11}	0.210
Prasad et al [58]	135.0	1.69×10^8	1.000
	175.0	8.75×10^9	1.160
Pau et al [59]	179.0	3.61×10^{14}	9.510
	231.0	4.72×10^{16}	1.230
Present Work	59.8	2.45×10^4	1.905
	107.2	1.20×10^6	2.882

The presented results show that the obtained kinetics parameters (activation energies and pre-exponential factors) in the present work are the lowest compared to the the published ones. The difference between the kinetic parameters estimated in this study and those calculated by other workers may probably be attributed the fact that types of studied polyurethane are different.

335 The kinetic models used to describe polyurethane pyrolysis may also influence the obtained va-
336 lues kinetic parameters. Other factors include the experimental conditions of thermogravimetric
337 analysis and the calculation procedure used to determine the kinetic parameters can cause the
338 difference between the values of the estimated parameters.

7. Conclusion

339 A kinetic analysis for the polyurethane pyrolysis was conducted in this paper. Thermal ana-
340 lysis of the polyurethane was carried out with the thermogravimetry technique which allows a
341 non-isothermal determination of conversion ratio and conversion rate curves as a function of hea-
342 ting rate. Different experiments for polyurethane pyrolysis were conducted at different heating
343 rates. The experimental results showed that the polyurethane pyrolysis is mainly completed in
344 two steps, the first one takes place between 100 and 300 °C, and the second occurs between 300
345 and extends to 800 °C.

346 A kinetic model has been presented to describe solid matter pyrolysis during the TGA analy-
347 sis. This model is based on the parallel independent reactions models. In order to determine the
348 kinetic parameters of the different reactions of polyurethane pyrolysis, a nonlinear least-square
349 procedure has been used. The proposed model has been employed to describe the polyurethane
350 pyrolysis using two and four reactions. The results shows that the use of four reactions model
351 allowed to described more accurately the experimental data, particularly to reproduce the highly
352 overlapped reactions (shoulders). A comparison of the kinetic parameters calculated using the
353 sample and the furnace temperatures showed that thermal-lag can affect considerably the kine-
354 tic analysis. In order to improve the reliability of the kinetic analysis, one should minimize the
355 deviation between the sample and furnace temperature (thermal-lag). The kinetics parameters of
356 polyurethane pyrolysis estimated in the paper would be used later in CFD codes to simulate gas
357 emission occurring during casting process.

Acknowledgement

358 This study is fully-funded by Montupet SA. The authors would like to express their deep ack-
359 nowledgment to Montupet. We thank INERIS (Institut National de l'Environnement Industriel
360 et des RISques) for their technical support in TGA experiments. We are grateful to Dr. Vahid
361 Ebrahimian and M. Aghiles Garah for their help in this work. Finally, we thank the reviewers
362 whose thoughtful guidance helped to improve the manuscript.

- 363 [1] M. Divandari, J. Campbell, Mechanisms of bubble damage in castings, in : A. F. Society (Ed.), 1st International
 364 Conference on Gating, Filling and Feeding of Aluminum Castings : Oct. 11 - 13, 1999, Opryland Hotel, Nashville,
 365 TN, 1999, pp. 49–63.
- 366 [2] J. Campbell, Complete Casting Handbook : Metal Casting Processes, Techniques and Design, 1st Edition, ELSE-
 367 VIER, 2011.
- 368 [3] J. H. Flynn, L. A. Wall, General treatment of the thermogravimetry of polymers, *J Res Nat Bur Stand* 70 (6) (1966)
 369 487–523.
- 370 [4] R. Font, A. Fullana, J. Caballero, J. Candela, A. García, Pyrolysis study of polyurethane, *Journal of Analytical and*
 371 *Applied Pyrolysis* 58–59 (0) (2001b) 63 – 77.
- 372 [5] C. A. Lytle, W. Bertsch, M. D. McKinley, Determination of thermal decomposition products from a phenolic
 373 urethane resin by pyrolysis-gas chromatography-mass spectrometry, *Journal of High Resolution Chromatography*
 374 21 (2) (1998) 128–132.
- 375 [6] R. S. Dungan, J. B. Reeves III, Pyrolysis of foundry sand resins : A determination of organic products by mass
 376 spectrometry, *Journal of Environmental Science and Health, Part A* 40 (8) (2005) 1557–1567.
- 377 [7] Y. Wang, F. S. Cannon, M. Salama, J. Goudzwaard, J. C. Furness, Characterization of hydrocarbon emissions from
 378 green sand foundry core binders by analytical pyrolysis, *Environmental Science & Technology* 41 (22) (2007)
 379 7922–7927.
- 380 [8] G. Jomaa, Étude des dégagements gazeux survenant pendant la coulée de pièces d'aluminium, Ph.D. thesis,
 381 MINES-ParisTech, France (2014).
- 382 [9] J. Caballero, R. Font, M. Esperanza, Kinetics of the thermal decomposition of tannery waste, *Journal of Analytical*
 383 *and Applied Pyrolysis* 47 (2) (1998) 165 – 181.
- 384 [10] J. Park, S. Oh, H. Lee, H. Kim, K. Yoo, Kinetic analysis of thermal decomposition of polymer using a dynamic
 385 model, *Korean Journal of Chemical Engineering* 17 (5) (2000) 489–496.
- 386 [11] J. Conesa, A. Marcilla, J. Caballero, R. Font, Comments on the validity and utility of the different methods for
 387 kinetic analysis of thermogravimetric data, *Journal of Analytical and Applied Pyrolysis* 58-59 (0) (2001) 617 –
 388 633.
- 389 [12] R. Font, I. Martín-Gullón, M. Esperanza, A. Fullana, Kinetic law for solids decomposition. application to thermal
 390 degradation of heterogeneous materials, *Journal of Analytical and Applied Pyrolysis* 58–59 (0) (2001a) 703 – 731.
- 391 [13] R. Font, A. Marcilla, A. García, J. Caballero, J. Conesa, Comparison between the pyrolysis products obtained from
 392 different organic wastes at high temperatures, *Journal of Analytical and Applied Pyrolysis* 32 (0) (1995) 41 – 49.
- 393 [14] G. Várhegyi, M. J. A. Jr., E. Jakab, P. Szabó, Kinetic modeling of biomass pyrolysis, *Journal of Analytical and*
 394 *Applied Pyrolysis* 42 (1) (1997) 73 – 87.
- 395 [15] R. Rodríguez, D. Gauthier, S. Udaquiola, G. Mazza, O. Martinez, G. Flamant, R. J. LeBlanc, P. J. Loughton,
 396 R. Tyagi, Kinetic models for pyrolysis and combustion of sewage sludge, in : Conference, Proceedings on Moving
 397 Forward Wastewater Biosolids Sustainability : Technical, Managerial, and Public Synergy, GMSC, 2007, pp. 801–
 398 809.
- 399 [16] S. Hu, A. Jess, M. Xu, Kinetic study of chinese biomass slow pyrolysis : Comparison of different kinetic models,
 400 *Fuel* 86 (17-18) (2007) 2778 – 2788.
- 401 [17] Z. Li, W. Zhao, B. Meng, C. Liu, Q. Zhu, G. Zhao, Kinetic study of corn straw pyrolysis : Comparison of two
 402 different three-pseudocomponent models, *Bioresource Technology* 99 (16) (2008) 7616 – 7622.
- 403 [18] K. Miura, T. Maki, A simple method for estimating $f(e)$ and $k_0(e)$ in the distributed activation energy model, *Energy*
 404 *& Fuels* 12 (5) (1998) 864–869.
- 405 [19] S. Scott, J. Dennis, J. Davidson, A. Hayhurst, An algorithm for determining the kinetics of devolatilisation of
 406 complex solid fuels from thermogravimetric experiments, *Chemical Engineering Science* 61 (8) (2006) 2339 –
 407 2348.
- 408 [20] T. Sonobe, N. Worasuwannarak, Kinetic analyses of biomass pyrolysis using the distributed activation energy
 409 model, *Fuel* 87 (3) (2008) 414 – 421.
- 410 [21] J. Cai, R. Liu, New distributed activation energy model : Numerical solution and application to pyrolysis kinetics
 411 of some types of biomass, *Bioresource Technology* 99 (8) (2008) 2795 – 2799.
- 412 [22] G. Várhegyi, C. Honggang, G. Sandra, Thermal decomposition of wheat, oat, barley, and brassica carinata straws.
 413 a kinetic study, *Energy & Fuels* 23 (2) (2009b) 646–652.
- 414 [23] S. Vyazovkin, C. A. Wight, Isothermal and non-isothermal kinetics of thermally stimulated reactions of solids,
 415 *International Reviews in Physical Chemistry* 17 (3) (1998) 407–433.
- 416 [24] R. K. Agrawal, Analysis of non-isothermal reaction kinetics : Part 1. simple reactions, *Thermochimica Acta* 203 (0)
 417 (1992) 93 – 110.
- 418 [25] C. Popescu, Integral method to analyze the kinetics of heterogeneous reactions under non-isothermal conditions a
 419 variant on the ozawa-flynn-wall method, *Thermochimica Acta* 285 (2) (1996) 309 – 323.
- 420 [26] A. K. Galwey, M. E. Brown, Chapter 3 kinetic background to thermal analysis and calorimetry, in : M. E. Brown
 421 (Ed.), Principles and Practic, Vol. 1 of Handbook of Thermal Analysis and Calorimetry, Elsevier Science B.V.,

- 1998, pp. 147 – 224.
- [27] J. Zhang, L. Ge, X. Zhang, Y. Dai, H. Chen, L. Mo, Thermal decomposition kinetics of the Zn(II) complex with norfloxacin in static air atmosphere, *Journal of Thermal Analysis and Calorimetry* 58 (2) (1999) 269–278.
- [28] J. Órfão, F. Martins, Kinetic analysis of thermogravimetric data obtained under linear temperature programming—a method based on calculations of the temperature integral by interpolation, *Thermochimica Acta* 390 (1–2) (2002) 195 – 211.
- [29] L. Vlaev, I. Markovska, L. Lyubchev, Non-isothermal kinetics of pyrolysis of rice husk, *Thermochimica Acta* 406 (1-2) (2003) 1 – 7.
- [30] K. Chrissafis, Kinetics of thermal degradation of polymers, *Journal of Thermal Analysis and Calorimetry* 95 (1) (2009) 273–283.
- [31] A. Khawam, Application of solid-state kinetics to desolvation reactions, Ph.D. thesis (2007).
- [32] F. Yao, Q. Wu, Y. Lei, W. Guo, Y. Xu, Thermal decomposition kinetics of natural fibers : Activation energy with dynamic thermogravimetric analysis, *Polymer Degradation and Stability* 93 (1) (2008) 90 – 98.
- [33] N. Sbirrazzuoli, L. Vincent, A. Mija, N. Guigo, Integral, differential and advanced isoconversional methods : Complex mechanisms and isothermal predicted conversion–time curves, *Chemometrics and Intelligent Laboratory Systems* 96 (2) (2009) 219 – 226.
- [34] K. Słopiecka, P. Bartocci, F. Fantozzi, Thermogravimetric analysis and kinetic study of poplar wood pyrolysis, *Applied Energy* 97 (0) (2012) 491 – 497.
- [35] H. L. Friedman, Kinetics of thermal degradation of char-forming plastics from thermogravimetry. application to a phenolic plastic, *Journal of Polymer Science Part C : Polymer Symposia* 6 (1) (1964) 183–195.
- [36] H. E. Kissinger, Reaction kinetics in differential thermal analysis, *Analytical Chemistry* 29 (11) (1957) 1702–1706.
- [37] H. Anderson, A. Kemmler, R. Strey, Comparison of different non-linear evaluation methods in thermal analysis, *Thermochimica Acta* 271 (0) (1996) 23 – 29.
- [38] H. Anderson, R. Strey, A. Kemmler, D. Haberland, Effective search of starting values for kinetic parameters estimation, *Journal of thermal analysis* 49 (3) (1997) 1565–1569.
- [39] J. Opfermann, Kinetic analysis using multivariate non-linear regression. i. basic concepts, *Journal of Thermal Analysis and Calorimetry* 60 (2) (2000) 641–658.
- [40] G. Várhegyi, L. Pöppel, I. Földvári, Kinetics of the oxidation of bismuth tellurite, Bi_2TeO_5 : Empirical model and least squares evaluation strategies to obtain reliable kinetic information, *Thermochimica Acta* 399 (1–2) (2003) 225 – 239.
- [41] C. Reverte, J.-L. Dirion, M. Cabassud, Kinetic model identification and parameters estimation from {TGA} experiments, *Journal of Analytical and Applied Pyrolysis* 79 (1–2) (2007) 297 – 305.
- [42] C. Zhang, X. Jiang, L. Wei, H. Wang, Research on pyrolysis characteristics and kinetics of super fine and conventional pulverized coal, *Energy Conversion and Management* 48 (3) (2007) 797 – 802.
- [43] J. A. Conesa, A. Marcilla, R. Font, J. Caballero, Thermogravimetric studies on the thermal decomposition of polyethylene, *Journal of Analytical and Applied Pyrolysis* 36 (1) (1996) 1 – 15.
- [44] G. Várhegyi, P. Szabó, M. J. Antal, Kinetics of charcoal devolatilization, *Energy & Fuels* 16 (3) (2002) 724–731.
- [45] J. Caballero, J. Conesa, I. Martín-Gullón, R. Font, Kinetic study of the pyrolysis of neoprene, *Journal of Analytical and Applied Pyrolysis* 74 (1-2) (2005) 231 – 237.
- [46] J. Yan, H. Zhu, X. Jiang, Y. Chi, K. Cen, Analysis of volatile species kinetics during typical medical waste materials pyrolysis using a distributed activation energy model, *Journal of Hazardous Materials* 162 (2–3) (2009) 646 – 651.
- [47] M. G. Grønli, G. Várhegyi, C. Di Blasi, Thermogravimetric analysis and devolatilization kinetics of wood, *Industrial & Engineering Chemistry Research* 41 (17) (2002) 4201–4208.
- [48] D. Vamvuka, E. Kastanaki, M. Lasithiotakis, Devolatilization and combustion kinetics of low-rank coal blends from dynamic measurements, *Industrial & Engineering Chemistry Research* 42 (20) (2003) 4732–4740.
- [49] G. Várhegyi, Z. Sebestyén, Z. Czégény, F. Lezsóvit, S. Könczöl, Combustion kinetics of biomass materials in the kinetic regime, *Energy & Fuels* 26 (2) (2012) 1323–1335.
- [50] R. Hooke, T. A. Jeeves, “ direct search” solution of numerical and statistical problems, *J. ACM* 8 (2) (1961) 212–229.
- [51] V. Torczon, On the convergence of pattern search algorithms, *SIAM Journal on Optimization* 7 (1) (1997) 1–25.
- [52] M. J. Antal, G. o. Várhegyi, E. Jakab, Cellulose pyrolysis kinetics : revisited, *Industrial & engineering chemistry research* 37 (4) (1998) 1267–1275.
- [53] Y.-C. Lin, J. Cho, G. A. Tompsett, P. R. Westmoreland, G. W. Huber, Kinetics and mechanism of cellulose pyrolysis, *The Journal of Physical Chemistry C* 113 (46) (2009) 20097–20107.
- [54] R. E. Lyon, N. Safronava, J. Senese, S. I. Stoliarov, Thermokinetic model of sample response in nonisothermal analysis, *Thermochimica Acta* 545 (0) (2012) 82 – 89.
- [55] S. Vyazovkin, K. Chrissafis, M. L. D. Lorenzo, N. Koga, M. Pijolat, B. Roduit, N. Sbirrazzuoli, J. J. Suñol, {IC-TAC} kinetics committee recommendations for collecting experimental thermal analysis data for kinetic computations, *Thermochimica Acta* 590 (0) (2014) 1 – 23.

- 481 [56] A. K. Burnham, Obtaining reliable phenomenological chemical kinetic models for real-world applications, *Thermochimica Acta* 597 (0) (2014) 35 – 40.
482
- 483 [57] G. Rein, C. Lautenberger, A. C. Fernandez-Pello, J. L. Torero, D. L. Urban, Application of genetic algorithms
484 and thermogravimetry to determine the kinetics of polyurethane foam in smoldering combustion, *Combustion and
485 Flame* 146 (1–2) (2006) 95 – 108.
- 486 [58] K. Prasad, R. Kramer, N. Marsh, M. Nyden, T. Ohlemiller, M. Zammarano, Numerical simulation of fire spread on
487 polyurethane foam slabs, in : *Proceedings of the 11th international conference on fire and materials*. Interscience
488 Communications, London, 2009, pp. 697–708.
- 489 [59] D. S. Pau, C. M. Fleischmann, M. J. Spearpoint, K. Y. Li, Determination of kinetic properties of polyurethane foam
490 decomposition for pyrolysis modelling, *Journal of Fire Sciences* 31 (4) (2013) 356–384.